

## EXCESS MOLAR ISOBARIC HEAT CAPACITIES AND EXCESS MOLAR ENTHALPIES FOR WATER–DIMETHYLSULFOXIDE MIXTURES AT 25 °C

F. RODANTE and G. MARROSU

*Dipartimento di Ingegneria Chimica, dei Materiali, delle Materie Prime e Metallurgia, Università “La Sapienza”, Via del Castro Laurenziano 7. 00161 Roma (Italy)*

(Received 29 January 1988)

### ABSTRACT

Isobaric heat capacities and enthalpies of mixing for water–dimethylsulfoxide mixtures were measured at 25 °C. Excess thermodynamic functions,  $H^E$ ,  $C_p^E$ , and apparent molar capacities functions for both the components  $\Phi_{c,DMSO}$  and  $\Phi_{c,w}$ , were calculated over the molar function range. The excess heat capacity quantity shows a pronounced asymmetry with respect to the normal trend in the  $0.6 < X_{DMSO} < 0.7$  mole fraction range in which it seems that a structure change takes place. The enthalpies of mixing and the apparent molar capacities confirm the structure-maker effect of DMSO on water and the structure-breaker effect of water on DMSO.

### INTRODUCTION

The dimethylsulfoxide (DMSO)–water mixture is one of the most widely investigated because of the importance of its components. It is generally known that binary solutions can be conveniently classified on the basis of their thermodynamic molar excess functions [1]. The DMSO–water solutions fall into the class called typically non-aqueous (TNA) [1a] where  $|H^E| > |TS^E|$ , i.e. enthalpy controlled.

However, despite the numerous studies [2–15] of their thermodynamic properties, the interactions between DMSO and water are not yet fully understood. Because molar capacity values are very sensitive to structural changes in solution, and because the above cited solutions are enthalpy controlled, it seemed worthwhile investigating these properties over a complete mole fraction range.

### EXPERIMENTAL AND PROCEDURE

The DMSO (Carlo Erba) was distilled twice under dry nitrogen at reduced pressure after treatment with NaOH pellets for 2 h at 90 °C. The

water content, measured by Karl Fischer titration, was 90 p.p.m. Calorimetric apparatus and the measurements of the partial molar enthalpy solution of H<sub>2</sub>O and DMSO in water–solution mixtures have been described previously [12]. It is noteworthy that the calorimetric cell was filled with a volume (200 ml) of solution, twice as large with respect to those normally used. In this way it can be reasonably assumed that the solution composition does not change upon additions of small amounts (60–120 mg) of water and DMSO. For heat capacity measurements the following procedure was used.

A Tronac (model 458) calorimeter was used. This is a quasi-adiabatic calorimeter especially suitable for measuring the heat developed by reagents in the liquid phase. The calorimetric vessel was a rapid-response, glass vacuum dewar of 100 cm<sup>3</sup> maximum capacity. The thermostat was maintained at  $298.15 \pm 0.0002$  K by employing a Tronac PTC-41 precision temperature controller.

Potential versus time measurements were made using a Fluka 8810A digital voltmeter. A thermistor with a value of 1975 ohm at 25°C was used to measure the temperature change. The experimental calibration of the thermistor indicated that it follows the linear equation  $T = 3.16 \times 10^{-6}$  mV  $\pm$  25. The unbalance of the bridge was fed into a Hitachi 561-1000L/p strip-chart recorder and into the digital voltmeter which, in turn, was connected to an Olivetti M24 computer.

#### *Calculation of the isobaric heat capacity*

During an experiment carried out with a generic calorimeter, some heat will exchange between the calorimeter and its isothermal surrounding. This exchange follows Newton's cooling law

$$Q = K(T - T_e) dT \quad (1)$$

where  $T$  is the temperature of the outer surface of the reaction vessel,  $T_e$  is the temperature of the surrounding thermostatic bath (the jacket temperature), and  $K$  is the calorimetric leakage constant. The heat exchange is a function of heating by stirring, of resistance heating across the thermistor and of the heat leaks (heat losses by conduction, radiation, convection and evaporation).

The first two heat sources can be eliminated by substituting the temperature  $T_e$  with the constant temperature  $T_\infty$ , which the calorimetric vessel will approach after a very long time [16]. During this last, the "jacket temperature" must be constant and the stirrer and the current supply of the thermistor must be in operation. The method normally used for determining the heat capacity is based on the supply of known amounts of energy during the time  $t$  across the heater resistance  $R$ . From the resulting temperature change  $\Delta T$ , and using the expression

$$Q = C_p \Delta T \quad (2)$$

it is possible to calculate  $C_p$ . This method has two drawbacks: (1) the energy supplied in time  $t$  cannot be constant because the resistance values are a function of time; and (2) one must wait for the transition periods of the heat conduction to be completed before measuring the temperature change  $\Delta T$ . These factors mean that longer measuring times are required which, in turn, make it necessary to calculate, by means of the integral, the heat dissipated.

If an infinitesimal range of time  $dT$  is considered, eqn. (2) becomes

$$dQ = C_p dT \quad (3)$$

For each (at continuous running)  $dT$  infinitesimal time,  $dQ$  is equal to the instantaneous power ( $P$ ) supplied, minus the amount of heat dissipated at temperature  $T$ .

$$dQ = P dT - k(T - T_\infty) dT \quad (4)$$

dividing eqns. (3) and (4) by  $dT$  and equalizing, one obtains

$$C_p dT/dt = P - k(T - T_\infty) \quad (5)$$

and again

$$C_p = \frac{P - k(T - T_\infty)}{dT/dt}$$

In order to calculate  $C_p$ , a measure of the instantaneous power ( $P=Vt$ ), through the calibration current  $I$  and the potential drop  $V$  of the resistance is sufficient. The change in temperature with respect to the equilibrium temperature  $T_\infty$ , and the slope of the thermogram  $dT/dt$  are also required. The calculation of heat capacity is inserted in appropriate algorithms, with which it is possible to calculate the enthalpy variation in constant environment and adiabatic calorimeters [17,18]. As the  $C_p$  value calculated in this way is the heat capacity of the vessel and its contents, the heat capacity of the empty reaction vessel  $C_r$  is expressed by  $C_r = C_p - V\rho c_p$  where  $V$ ,  $\rho$  and  $c_p$  are the volume, the density and the specific heat ( $\text{cal g}^{-1} \text{ }^\circ\text{C}^{-1}$ ) of solution at the calibration temperature, respectively. Water (100 ml) was used to calculate the  $C_r$  value. All  $C_p$  values for the various solutions were calculated using a volume equal to 100 ml. These values were corrected by subtracting  $C_r$ .

## RESULTS AND DISCUSSION

The partial molar solution enthalpies of water  $\Delta\bar{H}_{\text{H}_2\text{O}}$  and dimethylsulfoxide  $\Delta\bar{H}_{\text{DMSO}}$  are given in Table 1 and plotted versus  $X_{\text{DMSO}}$  in Fig. 1. The heat isobaric capacity  $C_p$  and the mean heat molar isobaric capacity  $\bar{C}_p$  are reported in Table 2 and plotted in Fig. 2.

TABLE 1

The partial molar enthalpies of solution of water,  $\Delta\bar{H}_{\text{H}_2\text{O}}$ , and DMSO,  $\Delta\bar{H}_{\text{DMSO}}$ , in water–DMSO solutions of various mole fractions at 25°C

$X_{\text{DMSO}}$	$-\Delta\bar{H}_{\text{H}_2\text{O}}$ (cal mol <sup>-1</sup> )	$-\Delta\bar{H}_{\text{DMSO}}$ (cal mol <sup>-1</sup> )
0.00	0	4328
0.10	121	3334
0.20	292	2146
0.28	486	1378
0.35	686	760
0.40	865	532
0.50	1114	221
0.60	1263	70
0.70	1347	61
0.80	1360	38.5
0.90	1357	35
0.95	1322	21.7
1.00	1280	0

The enthalpies of mixing per mole for the solutions of various mole fractions were calculated using the partial molar enthalpy solution values in the expression

$$(\Delta\bar{H}_{\text{mix}})_X = X_{\text{DMSO}}\Delta\bar{H}_{\text{DMSO}} + (1 - X_{\text{DMSO}})\Delta\bar{H}_{\text{H}_2\text{O}} \quad (7)$$

This method of determining the values of the enthalpy of mixing was used to avoid the large temperature rise and consequent variation of heat capacity due to the direct mixing of a relatively large amount of the two liquids. The

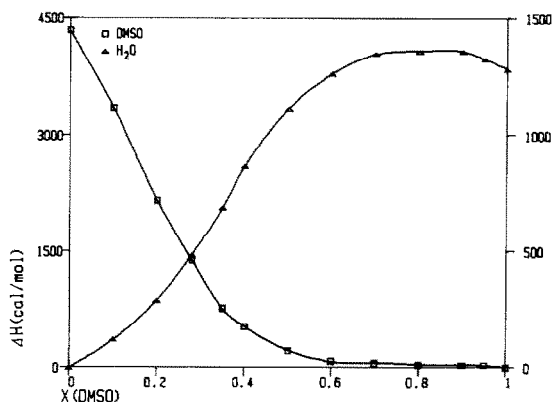


Fig. 1.  $\Delta\bar{H}_{\text{H}_2\text{O}}$  ( $\Delta$ ) and  $\Delta\bar{H}_{\text{DMSO}}$  ( $\square$ ) values in water–DMSO mixtures of various mole fractions at 25°C. The left-hand enthalpy scale is for  $\Delta\bar{H}_{\text{DMSO}}$ , and the right-hand enthalpy scale is for  $\Delta\bar{H}_{\text{H}_2\text{O}}$ .

TABLE 2

The isobaric heat capacity,  $C_p$ , and mean molar isobaric heat capacity,  $\bar{C}_p$ , of water–DMSO mixtures at 25 °C

$X_{\text{DMSO}}$	$C_p$ (cal K <sup>-1</sup> )	$\bar{C}_p$ (cal mol <sup>-1</sup> K <sup>-1</sup> )
0.00	100	18.00
0.10	85.11	20.48
0.20	79.85	23.97
0.30	73.12	26.39
0.40	67.26	28.38
0.50	62.51	30.05
0.60	57.70	31.19
0.70	58.05	34.97
0.80	55.03	36.44
0.90	50.72	36.60
1.00	46.00	36.72

maximum value of  $-\Delta\bar{H}_{\text{H}_2\text{O}}$  suggests that water–DMSO solution at  $X_{\text{DMSO}} = 0.8$  solvates water molecules slightly better than does pure DMSO.

As a proton donor species in DMSO can break the cyclic structure of the solvent, forming some linear aggregates [5,7], DMSO containing some water should present a less-ordered structure than does pure DMSO, becoming more available for the solvation of a subsequent small amount of added water. According to this hypothesis, water behaves towards DMSO as a structure breaker, while DMSO added in small amounts to water shows the properties of a structure maker. Indeed the sharp decrease of  $-\Delta\bar{H}_{\text{DMSO}}$  in

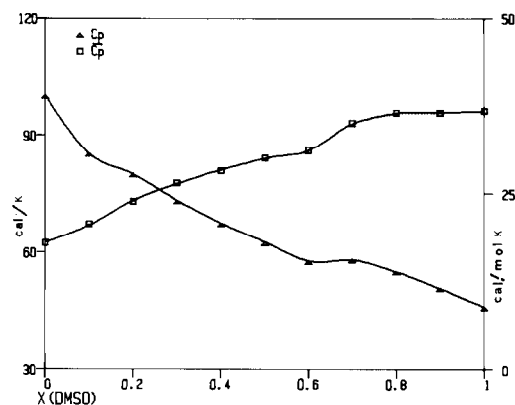


Fig. 2. The heat capacity  $C_p$  ( $\Delta$ ) for 100 g of DMSO–water mixtures and the molar mean  $\bar{C}_p$  heat capacity ( $\square$ ) of DMSO–water mixtures at 25 °C. The left-hand heat capacity scale is for  $C_p$  ( $\Delta$ ), and the right-hand heat capacity scale is for  $\bar{C}_p$  ( $\square$ ).

TABLE 3

The excess heat mean capacity,  $C_p^E$  and excess enthalpy of mixing  $H^E$ , for water–DMSO mixtures at 25 °C

$X_{\text{DMSO}}$	$C_p^E$ (cal mol <sup>-1</sup> K <sup>-1</sup> )	$H^E$ (cal mol <sup>-1</sup> )
0.00	0	0
0.10	0.61	442
0.20	2.23	663
0.28	–	736
0.30	2.77	–
0.35	–	746
0.40	2.89	731
0.50	2.69	667
0.60	1.96	547
0.70	3.87	447
0.80	3.46	303
0.90	1.75	168
0.95	–	87
1.00	0	0

water-rich solutions implies a hydrophobic effect of DMSO on water, with a consequent reinforcing of the water structure.

Thermodynamic properties of binary solvent mixtures are often described in terms of excess molar thermodynamic functions. Normally (with the exception of the free energy and the entropy values) these functions are defined as

$$P^E = \bar{P} - X_1 P_1^\ominus - X_2 P_2^\ominus$$

where  $\bar{P}$  is the mean molar quantity and  $P_1^\ominus$  and  $P_2^\ominus$  are the standard molar quantities of the two pure compounds.

As is well known, the enthalpy of mixing is coincident with the enthalpy excess  $H^E$ . The  $H^E$  and  $C_p$  values are given in Table 3.

The Redlich–Kister equation

$$H^E/X_{\text{DMSO}}(1 - X_{\text{DMSO}}) = \sum_{j=1}^n A_j(1 - 2X_{\text{DMSO}})^{j-1}$$

was fitted for enthalpy values. The coefficient of this equation,  $A_j$ , together with the standard deviation (s.d.) of the fit, are given in the legend to Fig. 3. The values of  $H^E$  are negative in the total mole fraction composition. This agrees with the fact that the DMSO–water mixture is a complex solution where the interactions between unlike molecules are stronger than those between like molecules.

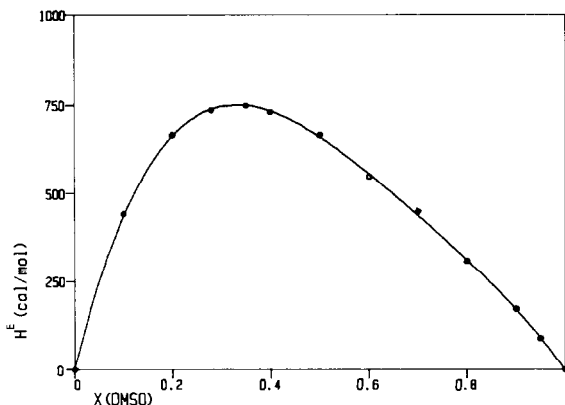


Fig. 3. The molar excess enthalpies,  $H^E$ , for water–DMSO mixtures versus the mole fraction of DMSO at 25°C. The  $A_j$  coefficient, the coefficient of correlation  $r$ , and the standard deviation s.d., of the fit for the least-squares representation by the equation  $H^E = X_{\text{DMSO}}(1 - X_{\text{DMSO}})\sum_{j=1}^n A_j(1 - 2X_{\text{DMSO}})^{j-1}$  where  $r = 0.9997$ ; s.d. = 23.67;  $A_0 = 2644.4$ ;  $A_1 = 1782.8$ ;  $A_2 = 1020.4$ ;  $A_3 = 206.4$ ;  $A_4 = 192.2$ .

The Redlich–Kister equation approaches very closely the  $H^E$  experimental values. As mentioned above, the molar heat capacity excess values are able to stress structural changes in solutions.

Table 3 shows how for the  $C_p^E$  experimental data there is a pronounced asymmetry with respect to the normal trend of excess heat capacity values. For this reason, the  $C_p^E$  data were divided into three parts:  $X_{\text{DMSO}} < 0.6$ ,  $X_{\text{DMSO}} > 0.7$  and  $0.6 < X_{\text{DMSO}} < 0.7$ . In the first two the  $C_p$  data were fitted to the following polynomial

$$C_p^E = \sum_{j=1}^m A_j X_{\text{DMSO}}^j$$

The  $A_j$  coefficients and the standard deviations are given in the legend to Fig. 4.

The experimental data for  $0.6 < X_{\text{DMSO}} < 0.7$  deviate remarkably from the smoothed curves interpolated from the concentration at both sides of the above range of mole fractions. Such a complicated curve has frequently been observed, e.g. when  $H^E$  was measured for a mixture undergoing phase separation. In that curve  $H^E$  varies linearly with  $x$  in the concentration range occurring during phase separations. For a DMSO–water mixture a linear dependence of  $H^E$  from the mole fraction beyond the  $X_{\text{DMSO}} = 0.5$  has also been found [4]. However, as heat and molar heat capacities are more closely related to the behavior of the molecules in the liquid phase, with a consequent connection with the local enhancement of concentration fluctuation, our attention was focused on the experimental values of these properties as a function of  $X_{\text{DMSO}}$  (Fig. 2). The plateau for the  $C_p$  values and the sharp enhancement for  $C_p$  values in the mole fraction range 0.6–0.7, lead to

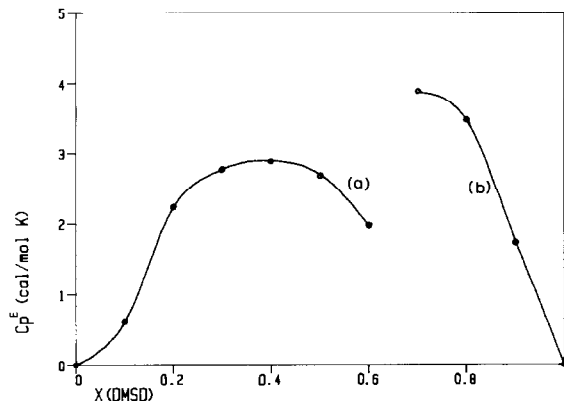


Fig. 4. The molar excess capacities of DMSO–water mixtures as a function of the mole fraction of DMSO at 25°C. The  $A_j$  coefficient, the coefficient of correlation  $r$ , and the standard deviation s.d. of the fit for the least squares representation by the equation  $C_p^E = \sum_{j=1}^n A_j X_{\text{DMSO}}^j$ . (a)  $X_{\text{DMSO}} < 0.6$ :  $r = 0.9832$ ; s.d. = 0.19;  $A_0 = -0.128$ ;  $A_1 = 11.4$ ;  $A_2 = -0.310$ ;  $A_3 = -21.7$ . (b)  $X_{\text{DMSO}} > 0.7$ :  $r = 0.9999$ ; s.d. =  $5 \times 10^{-3}$ ;  $A_0 = -131.8$ ;  $A_1 = 481.4$ ;  $A_2 = -553.4$ ;  $A_3 = 203.9$ .

a conviction that, in the above interval, a structural change which resembles a microphase separation or higher order transition occurs.

As is well known, apparent partial molar quantities are used to simplify the report of experimental data. It is possible to calculate the apparent molar heat capacity of component 2 (solute) from the relation

$$\Phi_c = \frac{\bar{C}_p - X_1 c_{p_1}^\ominus}{X_2}$$

where  $\bar{C}_p$  is the mean molar heat capacity and  $c_{p_1}^\ominus$  is the molar heat capacity of component 1 (solvent)

If  $\Phi_c$  is fitted with a polynomial equation in the mole fraction

$$\Phi_c = \sum_{j=1}^n A_j X_2^j$$

the  $\Phi_c^\ominus$  value (apparent molar heat capacity at infinite dilution, obtained by the extrapolation of experimental data) can be put equal to the partial molar heat capacity of the solute at infinite dilution  $\bar{c}_{p_2}^\ominus$ .

The difference between  $\bar{c}_{p_2}^\ominus$  and the pure molar heat capacity  $c_{p_2}^\ominus$  of the solute is often used as a criterion for the overall effects of the solute on the solvent. The values, at the various mole fractions, for both  $\Phi_{c,\text{DMSO}}$  and  $\Phi_{c,\text{H}_2\text{O}}$ , were calculated and fitted with the above polynomial equation. The  $A_j$  and  $S_j$  values are reported in the legends to Figs. 5 and 6, respectively.

The  $\Phi_{c,\text{DMSO}}$  pattern is reported in Fig. 5. The general trend of the apparent molar heat capacity is typical of a hydrophobic solute: first it increases with concentration and then drifts towards its molar value. The



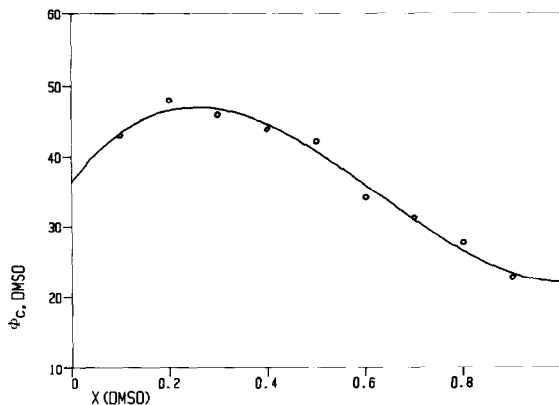


Fig. 5. The apparent molar heat capacities of DMSO,  $\Phi_{c, \text{DMSO}}$ , in water as a function of the mole fraction of DMSO at 25°C. The  $A_j$  coefficient, the coefficient of correlation  $r$ , and the standard deviation s.d., of the fit for the least-squares representation by the equation  $\Phi_{c, \text{DMSO}} = \sum_{j=1}^n A_j X_{\text{DMSO}}^j$ .  $r = 0.9921$ ; s.d. = 1.06;  $A_0 = 36.34$ ;  $A_1 = 91.15$ ;  $A_2 = -225.0$ ;  $A_3 = 119.4$ .

sharp decrease can be explained following the non-random two-liquid model (NRTL) in terms of contact pairing: the hydrophobic solutes lose part of their co-spheres on contact association. Moreover, the difference between  $\Phi_{c, \text{DMSO}}^{\ominus}$  and  $C_{\text{pDMSO}}^{\ominus}$  (which, as previously shown is used as a criterion for the overall effect of DMSO on water) is very small. This behavior is in agreement with the idea that structured organic solvents, such as NMF, dioxane and acetamide, are only weakly hydrophobic and have little overall

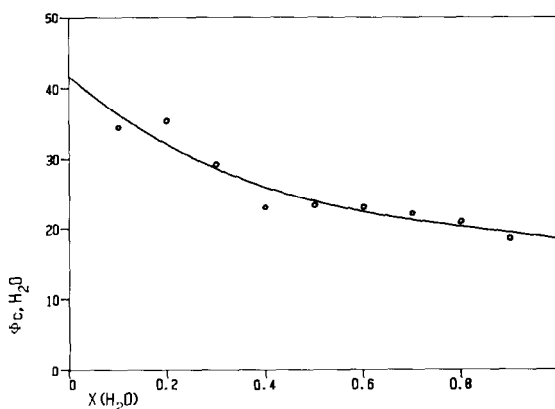


Fig. 6. The apparent molar heat capacities of water,  $\Phi_{c, \text{H}_2\text{O}}$  in DMSO as a function of the mole fraction of water at 25°C. The  $A_j$  coefficient, the coefficient of correlation  $r$ , the standard deviation s.d., of the fit for the least-squares representation by the equation  $\Phi_{c, \text{H}_2\text{O}} = \sum_{j=1}^n A_j X_{\text{DMSO}}^j$ .  $r = 0.9552$ ; s.d. = 1.68;  $A_0 = 41.66$ ;  $A_1 = -59.55$ ;  $A_2 = 59.21$ ;  $A_3 = -22.89$ .

influence on the water structure. Indeed, DMSO is a rather highly structured liquid, so that its molecule is slightly different from that of water.

The pattern of the  $\Phi_{c,w}$  values is reported in Fig. 6. The increasing value of  $\Phi_{c,w}$  on adding DMSO and the high difference value between  $C_{p_{H_2O}}^{\ominus}$  and  $\Phi_{c,w}^{\ominus}$  can be related to the hydrogen bonding between the  $H_2O$  molecules and the  $S=O$  group of DMSO. This also agrees with the large structure-breaking effect of small amounts of water on the DMSO structure.

## REFERENCES

- 1 A. Covington and P. Jones (Eds.), *Hydrogen-Bonded Solvent System*, Taylor and Francis, London: (a) F. Franks, p. 31; (b) B. Hyne, p. 99.
- 2 H.L. Clever and S. Pigott, *J. Chem. Thermodyn.*, 3 (1971) 221.
- 3 J. Kenttamaa and J.J. Lindberg, *Suom. Kemistil. B*, 33 (1960) 32.
- 4 J.J. Lindberg and J. Kenttamaa, *Suom. Kemistil. B*, 33 (1960) 104.
- 5 J. Kenttamaa and J.J. Lindberg, *Suom. Kemistil. B*, 33 (1960) 98.
- 6 W. Drinkard and D. Kivelson, *J. Phys. Chem.*, 62 (1968) 1494.
- 7 J.M.G. Cowie and P.M. Toporowski, *Can. J. Chem.*, 39 (1961) 2240.
- 8 E.M. Arnett and D.K. Mc Kelvey, *J. Am. Chem. Soc.*, 88 (1966) 2598.
- 9 J.J. Lindberg and C. Maiani, *Acta Chem. Scand.*, 17 (1963) 1477.
- 10 J.R. Holmes, D. Kivelson and W.C. Drinkard, *J. Am. Chem. Soc.*, (1962) 4677.
- 11 F. Rallo, F. Rodante and P. Silvestroni, *Thermochim. Acta*, 1 (1970) 311.
- 12 F. Rodante, F. Rallo and P. Fiordiponti, *Thermochim. Acta*, 6 (1973) 369.
- 13 O. Kivohan, G. Perron and J.E. Desnoyers, *Can. J. Chem.*, 53 (1975) 3263.
- 14 I. Horsak and I. Slama, *Collect. Czech. Chem. Commun.*, 48 (1987) 1936.
- 15 F. Rodante and A. Onofri, *Thermochim. Acta*, 94 (1985) 239.
- 16 F. Rodante and R. Rosati, *Thermochim. Acta*, 117 (1987) 167.
- 17 F. Rodante, A. Onofri and P. Perticaroli, *Thermochim. Acta*, 124 (1988) 185.
- 18 A.J. Parker, *Q. Rev. Chem. Soc.*, 16 (1962) 163.